

## Electronic Supplementary Information

For

### Mesogenic behavior of a 6-oxoverdazyl diradical: Towards organic high-spin liquid crystals

Szymon Kapuściński,<sup>a</sup> Jacek Szczytko,<sup>b</sup> Damian Pociecha,<sup>c</sup> and Piotr Kaszyński<sup>\*a,d,e</sup>

<sup>a</sup> Faculty of Chemistry, University of Łódź, Tamka 12, 91-403 Łódź, Poland

<sup>b</sup> Faculty of Physics, University of Warsaw, Pasteura 5, 02-093 Warsaw, Poland

<sup>c</sup> Faculty of Chemistry, University of Warsaw, Żwirki i Wigury 101, 02-089 Warsaw, Poland

<sup>d</sup> Organic Materials Research Group, Centre of Molecular and Macromolecular Studies, Polish Academy of Sciences, Sienkiewicza 112, 90-363 Łódź, Poland

<sup>e</sup> Department of Chemistry, Middle Tennessee State University, Murfreesboro, TN, 37130, USA

#### Table of Content:

1. NMR spectra	.....S2
2. VT EPR spectroscopy and data analysis for <b>4</b>	.....S3
a) sample preparation of diradical <b>4</b> in polystyrene ( <b>PS-4</b> )	.....S3
b) recording spectra for <b>PS-4</b>	.....S3
c) data analysis	.....S6
3. Magnetization measurements and data analysis for <b>4</b>	.....S6
4. Binary mixtures	.....S11
a) preparation of binary mixtures	.....S11
b) thermal analysis of binary mixtures	.....S11
c) additional optical textures of binary mixtures	.....S15
d) powder XRD measurements	.....S15
5. Computational details	.....S17
a) geometry optimization and PES scan	.....S17
b) singlet–triplet energy gap $\Delta E_{S-T}$	.....S18
6. Archive for DFT results	.....S19
7. References	.....S22

# 1. NMR spectra

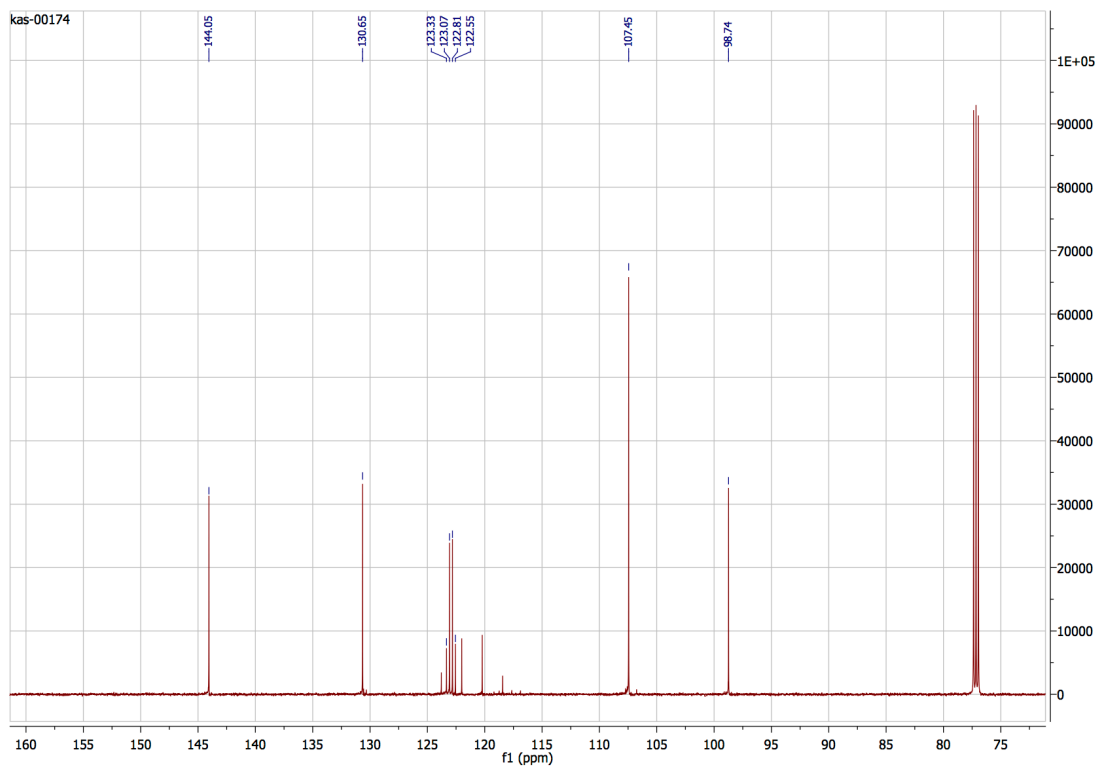
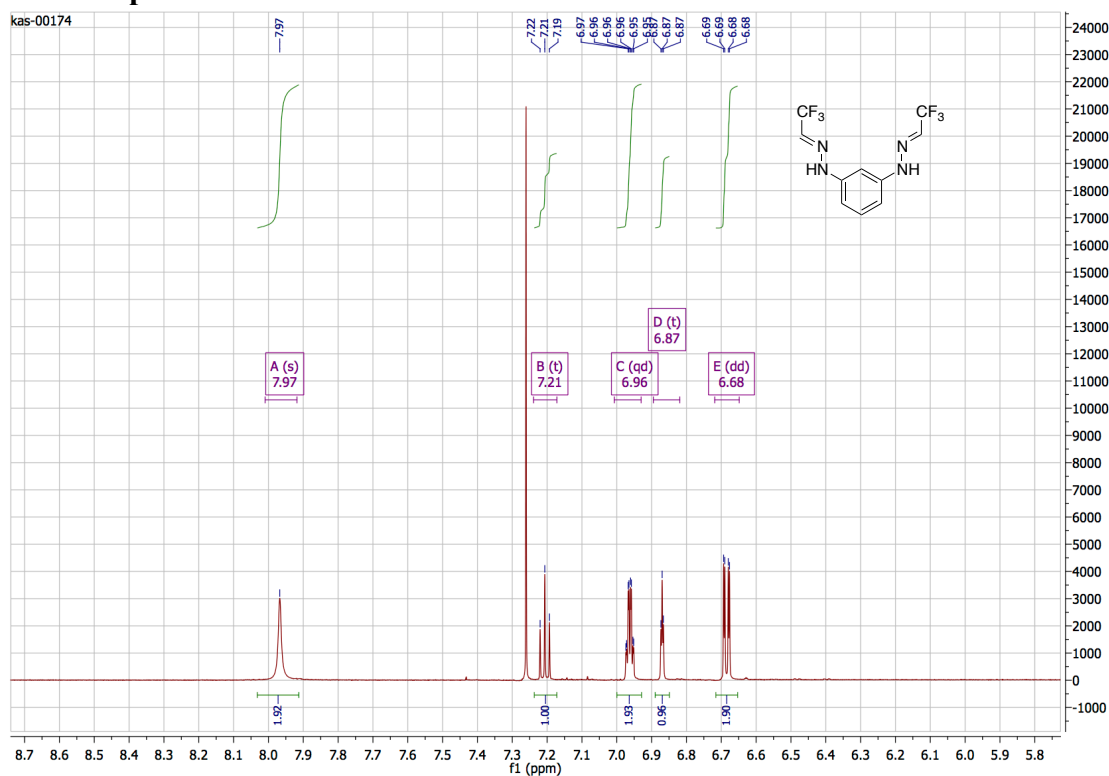


**Figure S1.**  $^1\text{H}$  NMR (600 MHz) and  $^{13}\text{C}\{^1\text{H}\}$  NMR (150 MHz) spectra of **6** ( $\text{CDCl}_3$ ).

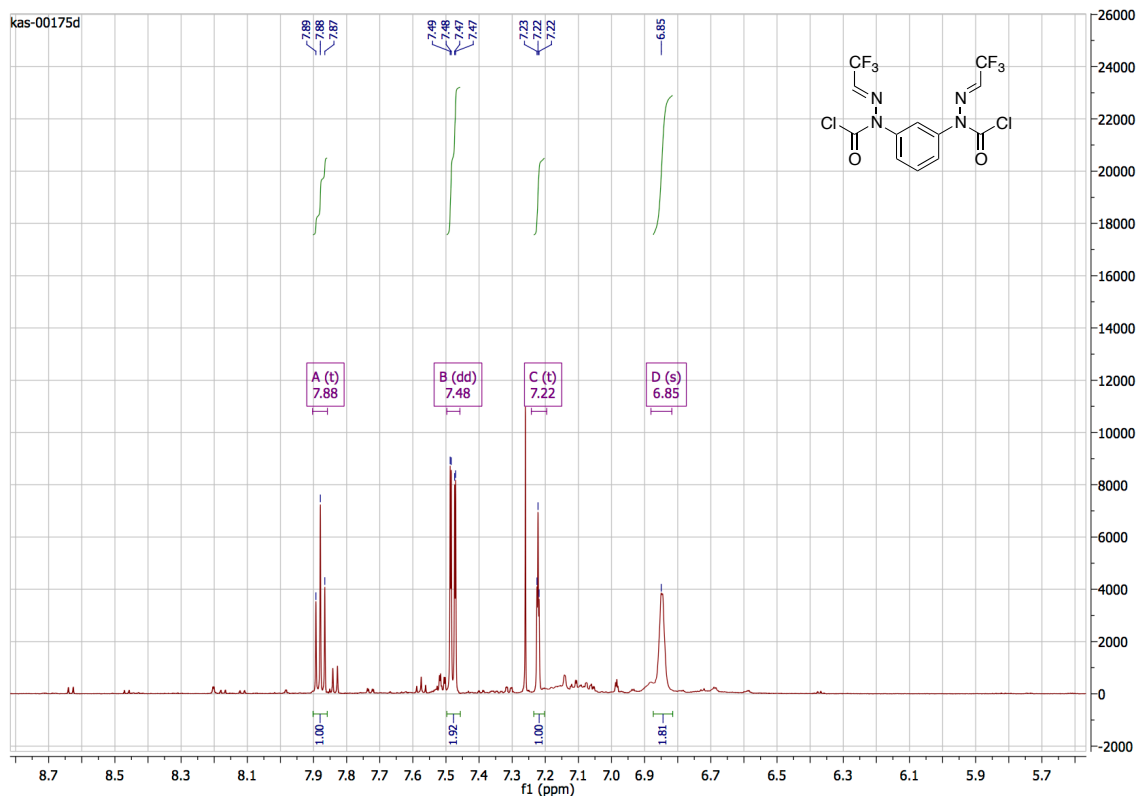


**Figure S2.** <sup>1</sup>H NMR (600 MHz) spectrum of crude biscarbamoyl chloride **7** (CDCl<sub>3</sub>).

## 2. VT EPR spectroscopy and data analysis

### a) sample preparation of diradical **4** in polystyrene PS-4

Diradical **4** (1.929 mg) and polystyrene (500.2 mg) were dissolved in CHCl<sub>3</sub> and poured into a small Petri dish to evaporate the solvent until a flexible, soft material was obtained. The material was placed in a flask and dried in vacuum at ambient temperature. The flask was evacuated and opened to argon (3×) and the resulting sample was stored under Ar. The dried polystyrene solid solution was placed in an EPR tube with help of a thin glass rod to fill the tube's space completely and degassed before the measurement.

### b) recording spectra for PS-4

EPR spectra for diradical **4** in polystyrene (**PS-4**) in a concentration of 5.25 mM were recorded on an X-band EMX-Nano EPR spectrometer in a temperature range 123–312 K with an interval of 5 K and tolerance of ±5 K. The microwave power was established with the Power Sweep program below the saturation of the signal, which was 25 dB or 0.3162

mW, modulation frequency of 100 kHz, modulation amplitude of 2 G, center field of 3440.4 G and spectral width of 400 G. Accurate  $g$ -values were obtained using TEMPO as EMX-Nano internal standard. EPR spectrum recorded at 123 K is shown in Figure S3, while selected spectra recorded in the full temperature range are presented in Figure S4.

Each EPR spectrum was double integrated and the resulting values are listed in Table S1 and shown graphically in Figure S5.

**Table S1.** Double integral and normalized data for **PS-4**.

Temp /K	DI	DI/DI <sub>123</sub>	DI <sub>rel</sub> •T	Temp /K	DI	DI/DI <sub>123</sub>	DI <sub>rel</sub> •T
123	9410	1.0000	123.00	217	51500	0.54729	118.76
127	90200	0.95855	121.74	222	50200	0.53348	118.43
132	86300	0.91711	121.06	227	49100	0.52179	118.45
136	83100	0.88310	120.10	232	47700	0.50691	117.60
142	79600	0.84591	120.12	237	46600	0.49522	117.37
147	77200	0.82040	120.60	242	45800	0.48672	117.79
152	74500	0.79171	120.34	247	44700	0.47503	117.33
157	72200	0.76727	120.46	252	43500	0.46227	116.49
162	69900	0.74283	120.34	257	42900	0.45590	117.17
167	67800	0.72051	120.33	262	42100	0.44740	117.22
172	65800	0.69926	120.27	266	41300	0.43889	116.75
176	64000	0.68013	119.70	272	40300	0.42827	116.49
182	61900	0.65781	119.72	276	39500	0.41977	115.86
187	60200	0.63974	119.63	281	38800	0.41233	115.86
192	58500	0.62168	119.36	287	37800	0.40170	115.29
197	57000	0.60574	119.33	291	37400	0.39745	115.66
202	55400	0.58874	118.92	296	36700	0.39001	115.44
207	54100	0.57492	119.01	302	35900	0.38151	115.22
212	52700	0.56004	118.73	307	35300	0.37513	115.17
				312	34800	0.36982	115.38

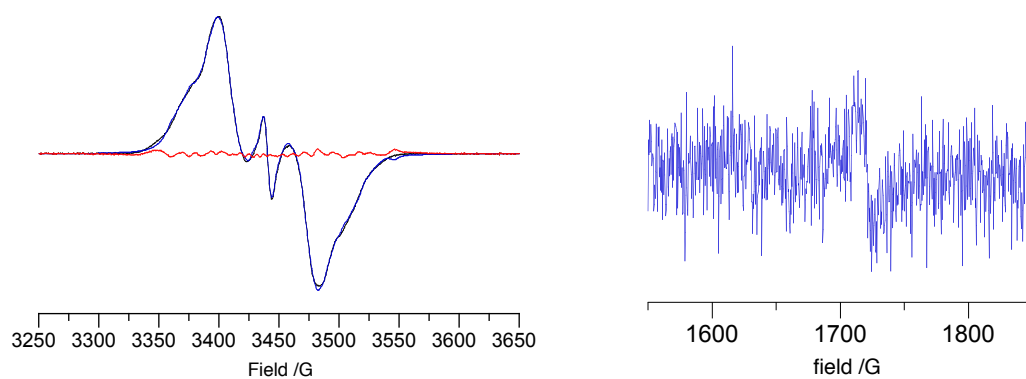


**Figure S3.** Left: EPR spectrum for diradical **4** in polystyrene (**PS-4**,  $c = 5.25$  mM) recorded at 123 K (black), simulated spectrum (blue) and residual (red). Right: Half-field transition in the same sample.

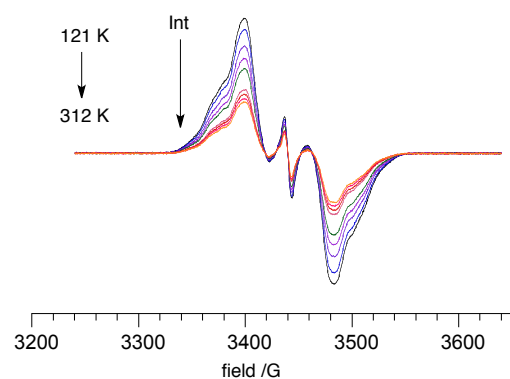


**Figure S4.** Decrease of intensity of the EPR spectrum for diradical **4** in polystyrene (**PS-4**,  $c = 5.25$  mM) with increasing temperature.

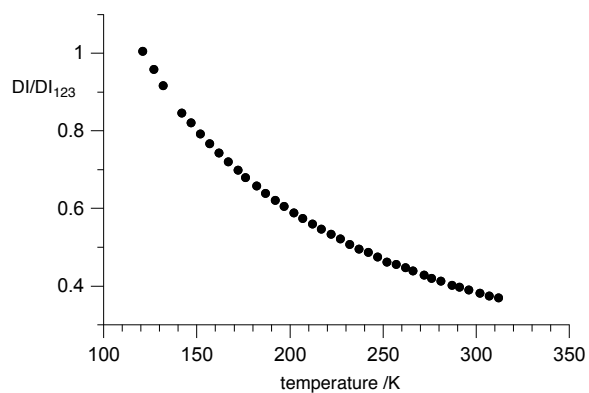


**Figure S5.** Relative double integral of the EPR spectra ( $DI_{rel} = DI/DI_{123}$ ) vs temperature for diradical **4** in polystyrene (**PS-4**,  $c = 5.25$  mM).

### *c) data analysis*

Simulations of the anisotropic spectrum recorded for solid solution **PS-4** at 123 K was performed with the EMX-Nano software using *Aniso-SpinFit* option. To account for the signal of a monoradical contamination at the center of the spectrum, simulation was performed with two species representing a diradical (triplet) and monoradical (doublet). Simulation results are shown below:

#### *Species 1 (triplet):*

Population: 68854.8

$g_{xx} = 2.00231$ ,  $g_{yy} = 2.00285$ ,  $g_{zz} = 2.00223$ ,

$zfs\ D = 190.23\ \text{MHz} = 6.345 \times 10^{-3}\ \text{cm}^{-1}$ ,  $zfs\ E = -4.24\ \text{MHz} = -1.41 \times 10^{-4}\ \text{cm}^{-1}$ .

lineshape = 0.6, linewidth x = 10.7599, linewidth y = 20.7346, linewidth z = 8.93406,

nitrogen nuclei:

N1:  $A_x = -11.4039\ \text{MHz}$ ,  $A_y = 18.0094\ \text{MHz}$ ,  $A_z = -4.7832\ \text{MHz}$

N2:  $A_x = -24.4428\ \text{MHz}$ ,  $A_y = 52.8243\ \text{MHz}$ ,  $A_z = 24.4685\ \text{MHz}$

#### *Species 2 (doublet):*

Population: 2171.9

$g_{xx} = 2.01242$ ,  $g_{yy} = 1.98167$ ,  $g_{zz} = 2.00336$ ,

$zfs\ D = 190.23$ ,  $zfs\ E = -4.24$ ,

lineshape = 0.6, linewidth x = 5.54084, linewidth y = 5.36955, linewidth z = 5.006,

nitrogen nuclei:

N1:  $A_x = 30.6074\ \text{MHz}$ ,  $A_y = 52.0368\ \text{MHz}$ ,  $A_z = 29.0084\ \text{MHz}$

N2:  $A_x = 34.5446\ \text{MHz}$ ,  $A_y = -16.5654\ \text{MHz}$ ,  $A_z = 31.3194\ \text{MHz}$

### **3. Magnetization measurements and data analysis for 4**

A microcrystalline sample of **4** ( $m = 12.10\ \text{mg}$ ,  $15.66 \times 10^{-6}\ \text{mol}$ ,  $M_w = 772.7\ \text{g mol}^{-1}$ ) was placed in a polycarbonate capsule fitted in a plastic straw and its magnetic susceptibility was measured as a function of temperature in cooling (300 K  $\rightarrow$  2 K) and heating (2 K  $\rightarrow$  400 K) modes at a rate of  $1\ \text{K min}^{-1}$  at 0.6 T, using a SQUID magnetometer (Quantum Design MPMS-XL-7T). Measurements of magnetization  $M$  *vs* applied field  $H$  were conducted at 2 and 300 K.

The magnetic effect of the capsule (scaled by the mass of the capsule) was subtracted from the raw data for the sample using the following method. For a given temperature  $T$  and magnetic field  $B$  magnetization  $M(B,T)$  was measured. Raw data

collected by SQUID magnetometer at each such a point are the electric signals  $U(x)$  measured as a function of sample position  $x$  in the SQUID pick-up coil (so called second-order gradiometer, Figure S6). The raw signal of empty polycarbonate capsule  $U_c(x)$  was measured independently as a function of temperature and magnetic field. For each measured raw data point  $U(x)$ , signal of the empty polycarbonate capsule,  $U_c(x)$ , was subtracted. The resulting difference of signals,  $U(x) - U_c(x)$ , was fitted to an analytical function provided by Quantum Design MPMS (Application Note 1014-213 <https://www.qdusa.com/sitedocs/appNotes/mpms/1014-213.pdf>), which gave a magnetic moment value  $M$ . This procedure was applied for each experimental data point to obtain  $M(T)$  and  $M(B)$  values and executed using an algorithm written in MatLab program (version R2019a). The corrected data of magnetization of the sample was used for further analysis.

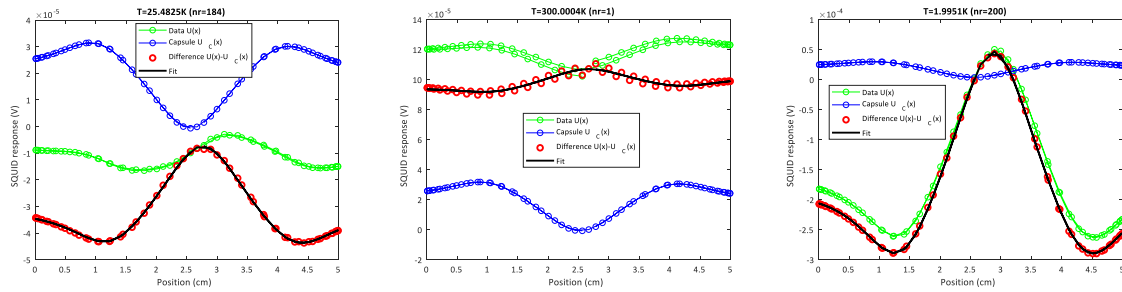


**Figure S6.** Examples of analysis of raw data: a)  $U(x) < U_c(x)$ , b)  $U(x) \sim U_c(x)$  (magnetic moment crosses 0 line); c)  $U(x) > U_c(x)$ .

Analysis of magnetization data obtained for **4** as described above was performed by calculating molar total magnetic susceptibility,  $\chi_{tot}$ , and subsequently establishing diamagnetic correction,  $\chi_{dia}$  from the linear portion of the  $\chi_{tot} \cdot T(T)$  plot to calculate the paramagnetic component,  $\chi_p$ , of the magnetic susceptibility.

The diamagnetic correction for the sample was estimated from the linear portion of high temperature  $\chi_{tot} \cdot T$  vs  $T$  plot assuming ideal paramagnetic behavior of the sample using the Curie law (eq 1).

$$\chi_{tot} \cdot T = (\chi_p + \chi_{dia}) \cdot T = C + \chi_{dia} \cdot T \quad (\text{eq 1})$$

where  $C = 0.375 \text{ cm}^3 \text{ mol}^{-1} \text{ K}$  for an ideal paramagnet ( $S = 1/2$ ).

A plot of a total molar magnetic susceptibility  $\chi_{\text{tot}}$  vs temperature for **4** is shown in Figure S7 and  $\chi_{\text{tot}} \cdot T$  (T) plot in Figure S8.

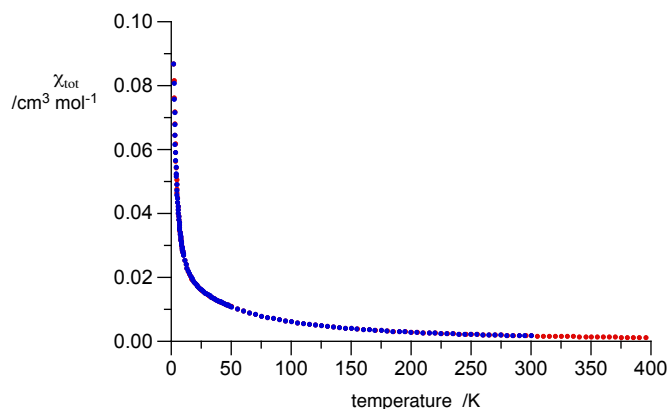


**Figure S7.** Total molar magnetic susceptibility  $\chi_{\text{tot}}$  of **4** vs T on cooling 300→2 K (blue) and on heating 2→400 K (red) at 0.6 T.

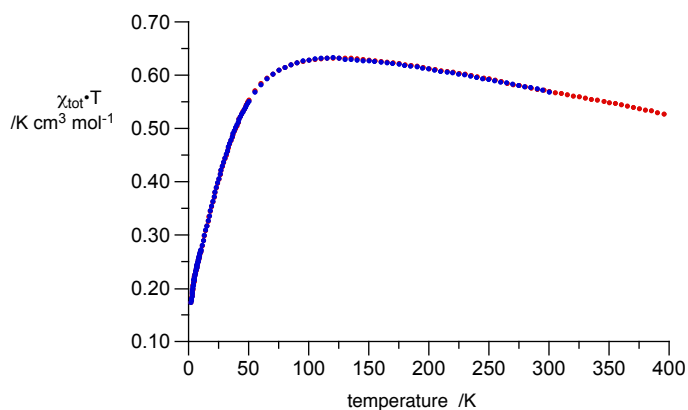


**Figure S8.** Total molar magnetic susceptibility  $\chi_{\text{tot}} \cdot T$  of **4** vs T on cooling 300→2 K (blue) and on heating 2→400 K (red) at 0.6 T.

The diamagnetic correction,  $\chi_{\text{dia}}$ , was determined with the Curie law as  $-4.37(2) \times 10^{-4} \text{ cm}^3 \text{ mol}^{-1}$  from a linear portion of the  $\chi_{\text{tot}} \cdot T$  vs T plots (Figure S8) in the temperature range 200 K – 400 K for the heating mode (Figure S9). The  $\chi_{\text{dia}}$  component of **4** calculated from Pascal constants<sup>1</sup> is  $-3.69 \times 10^{-4} \text{ cm}^3 \text{ mol}^{-1}$ .

The  $\chi_{\text{p}}$  vs T and  $\chi_{\text{p}} \cdot T$  vs T plots are shown in Figures S10 and S11.



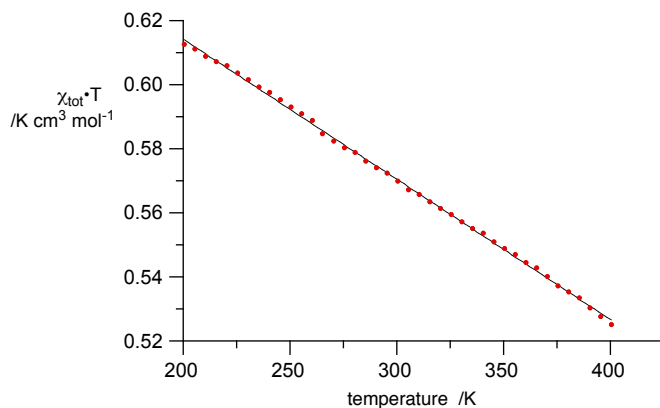


**Figure S9.** A linear portion of the  $\chi_{\text{tot}} \cdot T$  vs  $T$  plot for **4** (Figure S8) in a range of 200 K  $\rightarrow$  400 K. Best fit line:  $\chi_{\text{tot}} \cdot T = -0.000437(2) \cdot T + 0.702(1)$ ,  $r^2 = 0.999$ .

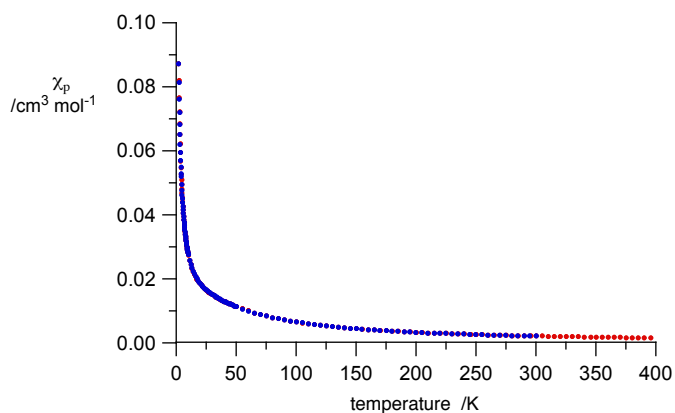


**Figure S10.** A  $\chi_p$  vs  $T$  plot for **4** in cooling (blue) and heating (red) runs with diamagnetic correction  $\chi_{\text{dia}} = -4.37 \times 10^{-4} \text{ cm}^3 \text{ mol}^{-1}$ .

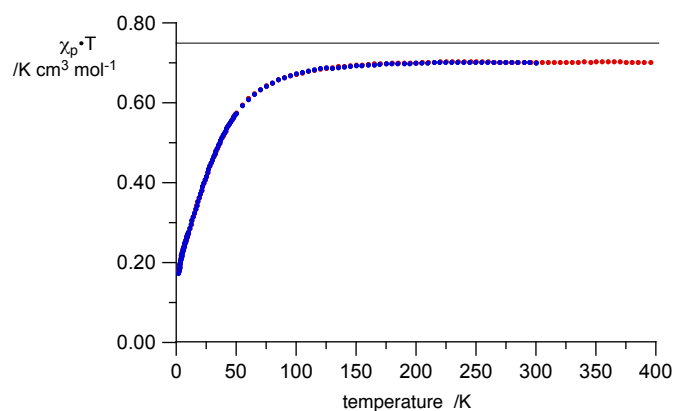


**Figure S11.** A  $\chi_p \cdot T$  vs  $T$  plot for **4** in cooling (blue) and heating (red) runs with diamagnetic correction  $\chi_{\text{dia}} = -4.37 \times 10^{-4} \text{ cm}^3 \text{ mol}^{-1}$ . The horizontal line marks the value of  $0.75 \text{ cm}^3 \text{ mol}^{-1} \text{ K}$  for two spins  $1/2$ .

Analysis of the  $1/\chi_p$  vs T plot (Figure S12) according to eq 2 gives  $C = 0.708 \text{ cm}^3 \text{ mol}^{-1} \text{ K}$  and  $\theta = -3.1(3) \text{ K}$ .

$$1/\chi_p = T \cdot 1/C - \theta/C \quad (\text{eq 2})$$

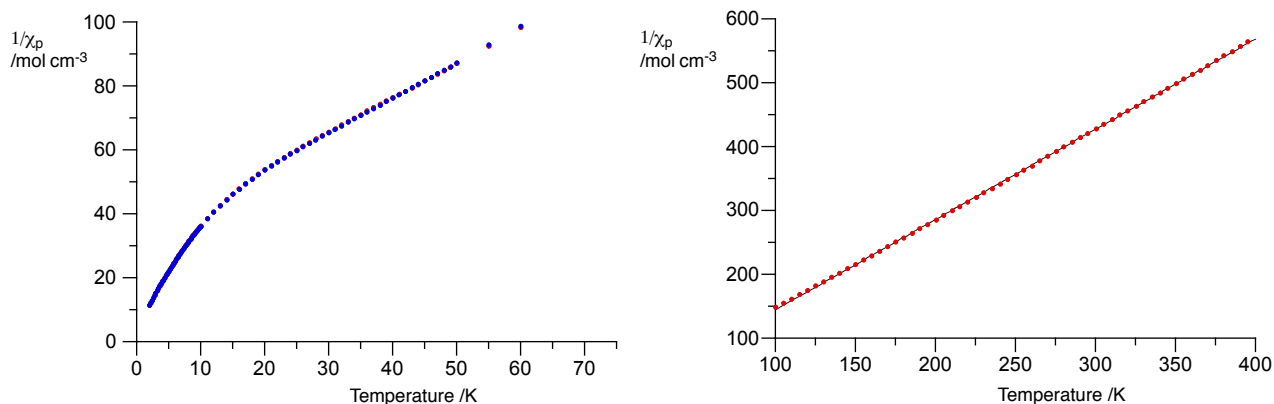


**Figure S12.** A  $1/\chi_p$  vs T plot for **4** in two temperature ranges for cooling (blue) and heating runs (red). The best-fit function from the high temperature plot (right):  $1/\chi_p = T \cdot 1.412(2) + 4.36(44)$ ,  $r^2 = 0.9999$ .

Molar paramagnetic magnetization,  $M_p$ , for **4** was obtained by subtracting the diamagnetic component of magnetization  $\chi_{\text{dia}} \cdot B$  (eq 3), where  $\chi_{\text{dia}} = -4.37 \times 10^{-4} \text{ cm}^3 \text{ mol}^{-1}$  and the field is in Oe. The resulting curves  $M_p$  obtained at 300 K and at 2 K are shown in Figure S13.

$$M_p = M_{\text{tot}} - \chi_{\text{dia}} B \quad (\text{eq 3})$$

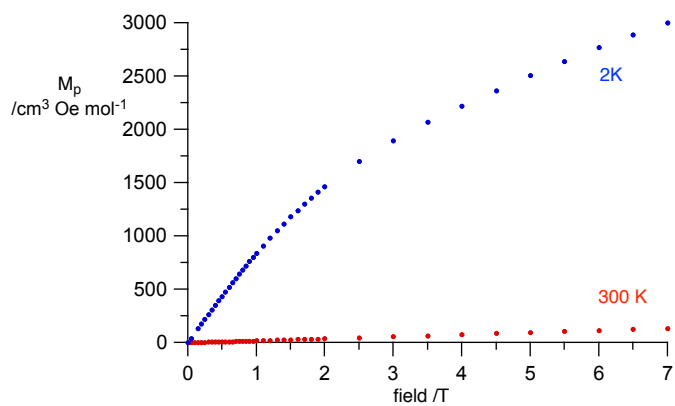


**Figure S13.** Molar paramagnetic magnetization  $M_p$  vs  $B$  for **4** at 2 K (blue) and at 300 K (red).

#### 4. Binary mixtures

##### *a) preparation of binary mixtures*

A mixture of known amounts of additive **2[6,6]** (~1  $\mu\text{mol}$ ) and the host (**1[8,6]** or **BT[6,8]**, ~10  $\mu\text{mol}$ ) was placed in a small vial and 1,2-dichloroethane (0.1 mL) was added. The mixture was heated and stirred with a spatula at 50 °C (hot stage) to give a homogenous solution. The solvent was removed under stirring at about 80 °C and the resulting mixture was analyzed by POM to confirm homogeneity.

##### *b) thermal analysis of binary mixtures*

Typically, each mixture was analyzed by a differential scanning calorimeter DSC-1 (Mettler Toledo) at a scanning rate of 10 K  $\text{min}^{-1}$ , in three heating-cooling cycles and reproducible results (within 0.5 K) were averaged. The resulting thermograms for each mixture are shown in Figures S14 and S15.

The resulting transition peak temperatures  $T_{\text{SmA-I}}$  were used to obtain virtual transition temperatures [ $T_{\text{SmA-I}}$ ] for the additive by linear extrapolation to  $x_i = 1$  with the intercept value set at the  $T_{\text{SmA-I}}$  for the pure host determined for the sample of the host used for the measurement. Results are collected in Table S2 and shown graphically in Figures S16 and S17.

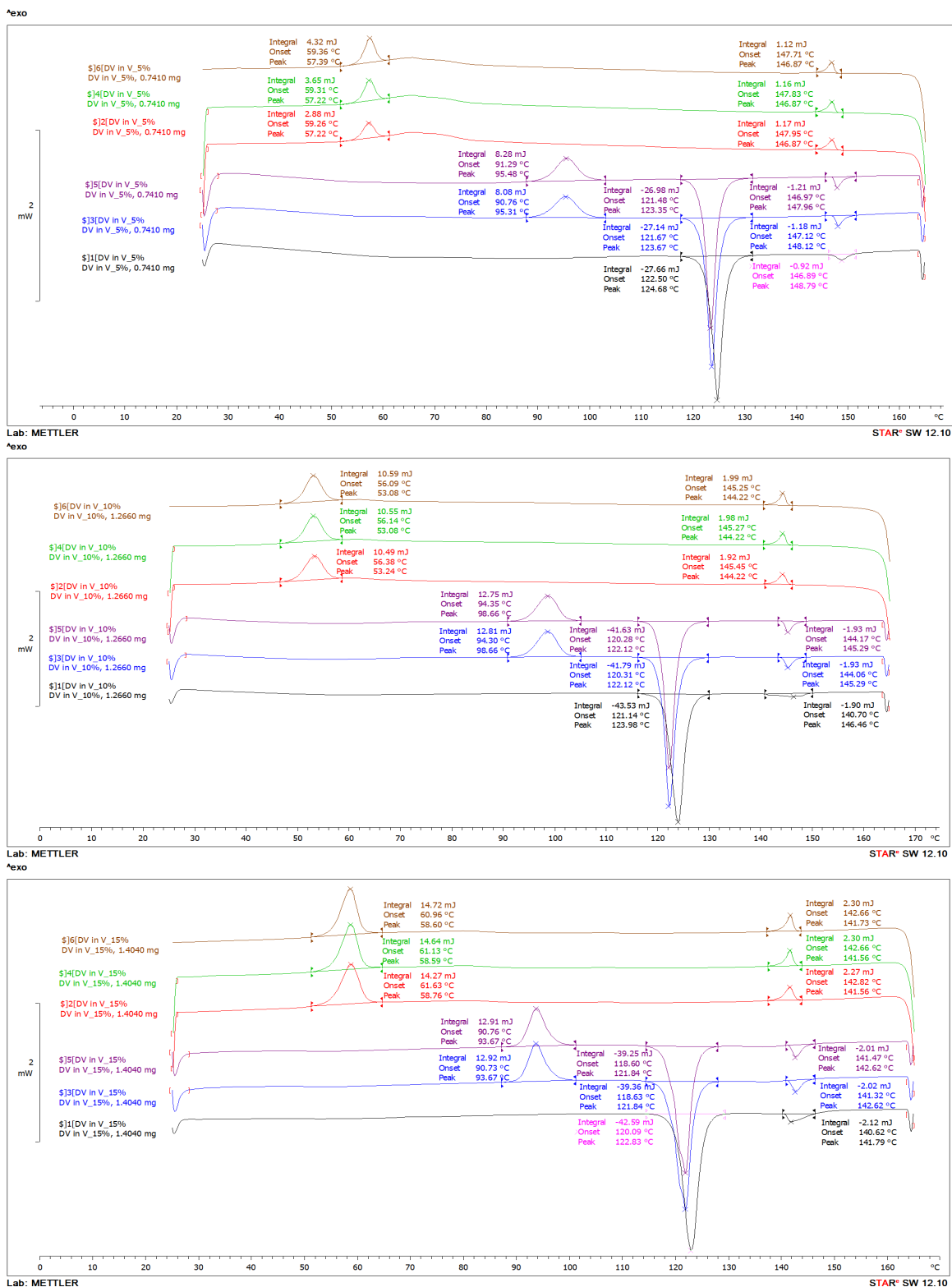
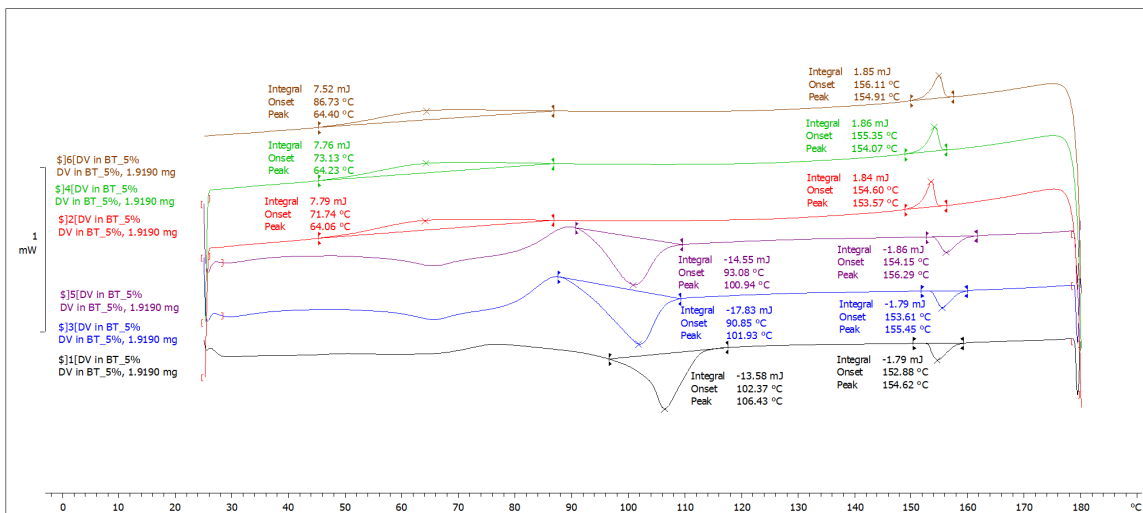
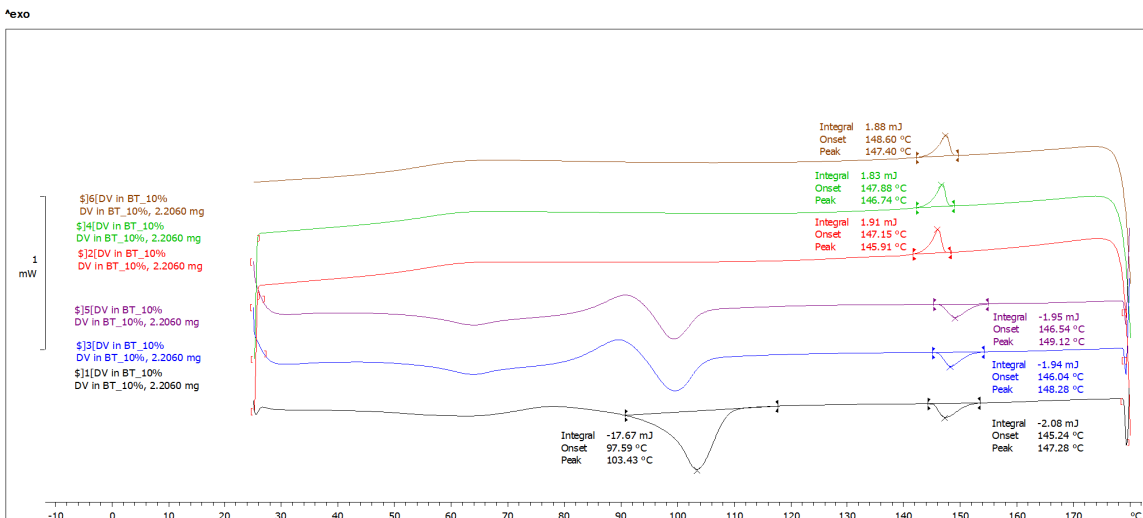


Figure S14. Differential Scanning Calorimetry (DSC) of binary mixtures (from the top) of 5, 10 and 15 mol% of 2[6,6] in host 1[8,6].

exo



exo



exo

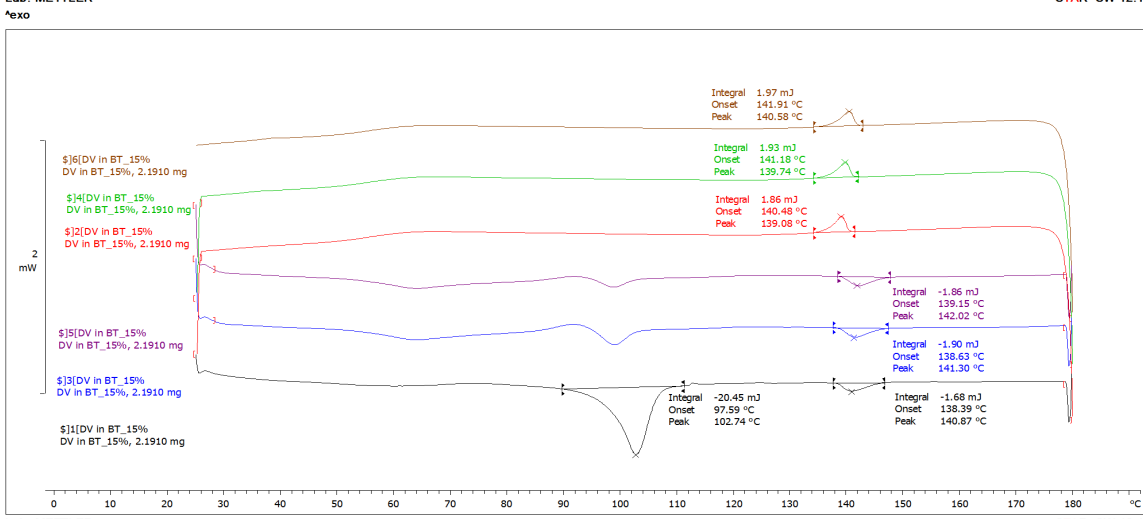


**Figure S15.** Differential Scanning Calorimetry (DSC) of binary mixtures (from the top) of 5, 10 and 15 mol% of 2[6,6] in host BT[6,8].

**Table S2.** Thermal properties for the pure components and for binary mixtures.

Pure host / °C	Binary mixtures		Virtual transition temperatures [ $T_{\text{SmA-I}}$ ] / °C
	mol %	SmA-I peak transition temperature / °C	
<b>1[8,6]</b>	0	149.3	<b>42 ± 3</b>
	5.01	148.1	
	10.06	145.3	
	15.04	142.6	
<b>BT[6,8]</b>	0	163.5	<b>7 ± 5</b>
	4.81	154.6	
	10.15	147.3	
	14.83	140.9	

• **2[6,6]** in host **1[8,6]**:

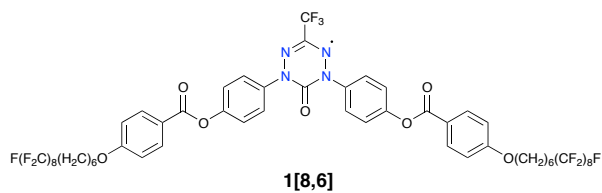
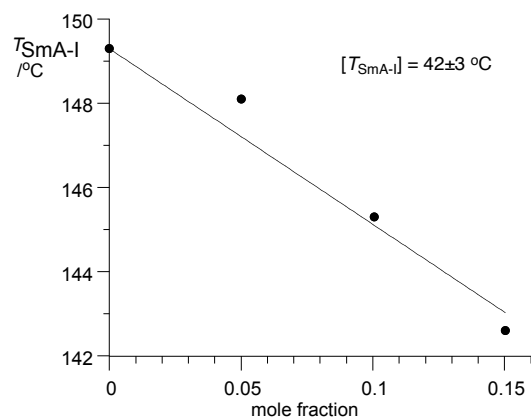


**Figure S16.** A plot of peak transition temperatures vs mole fraction for **2[6,6]** in host **1[8,6]**. Best fit function:  $T_{\text{SmA-I}} = 149.3 - 107.6(30) \times x_1$ ,  $r^2 = 0.962$ .

• **2[6,6]** in host **BT[6,8]**:

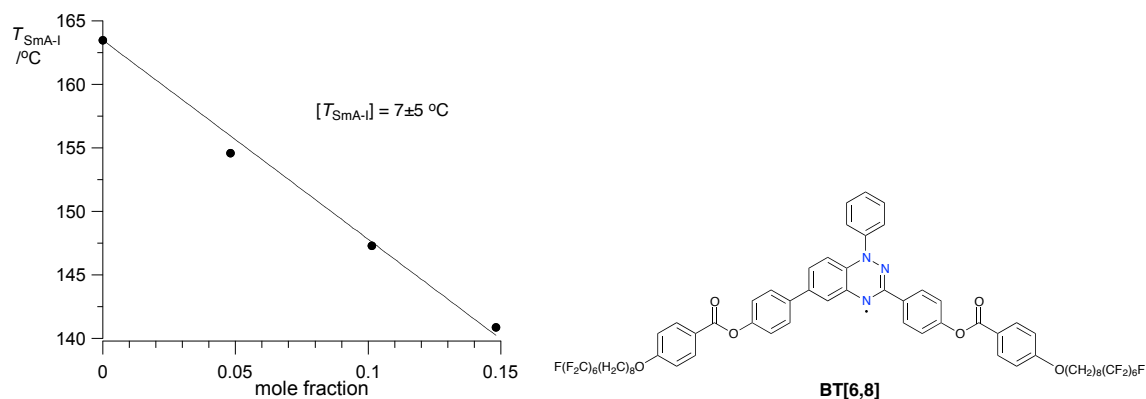


**Figure S17.** A plot of peak transition temperatures vs mole fraction for **2[6,6]** in host **BT[6,8]**. Best fit function:  $T_{\text{SmA-I}} = 163.5 - 156.7(48) \times x_1$ ,  $r^2 = 0.992$ .

*c) additional optical textures of binary mixtures*

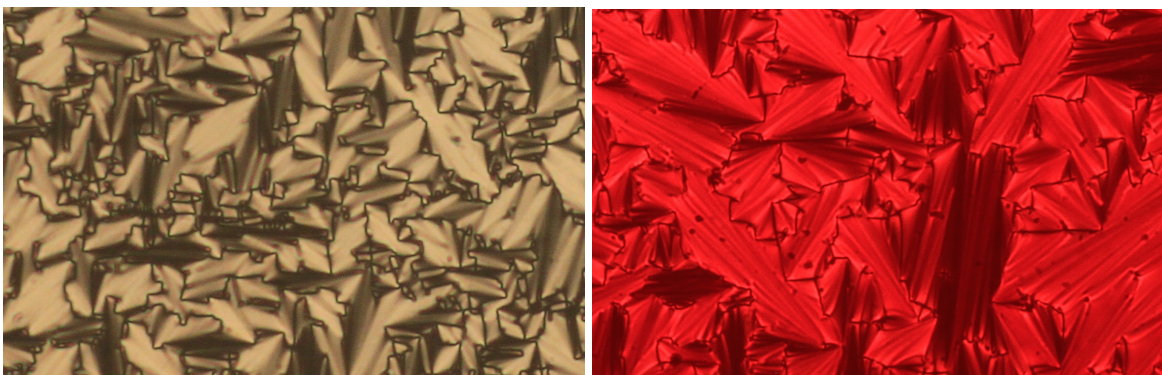


**Figure S18.** SmA optical textures obtained on cooling for 5 mol% of **2[6,6]** in host **1[8,6]** (left) and 5 mol% of **2[6,6]** in host **BT[6,8]** (right) and observed in polarized light.

*d) powder XRD measurements of binary mixtures*

X-ray diffraction experiments were conducted with Bruker D8 GADDS system, equipped with microfocus X-ray tube with Copper anode and dedicated X-ray optics, 0.5 mm point collimator and area detector Vantec 2000. Non-aligned (powder-like) or partially aligned samples of binary mixtures were prepared in a form of a droplet on a heated surface and thermostated with a modified Linkam heating stage. Recorded two-dimensional

diffraction patterns were integrated over azimuthal angle to obtain dependence of diffracted intensity on the diffraction angle  $2\theta$ . Results were analyzed with Bruker Topas software. Additional XRD results are shown in Figures S19 and S20.

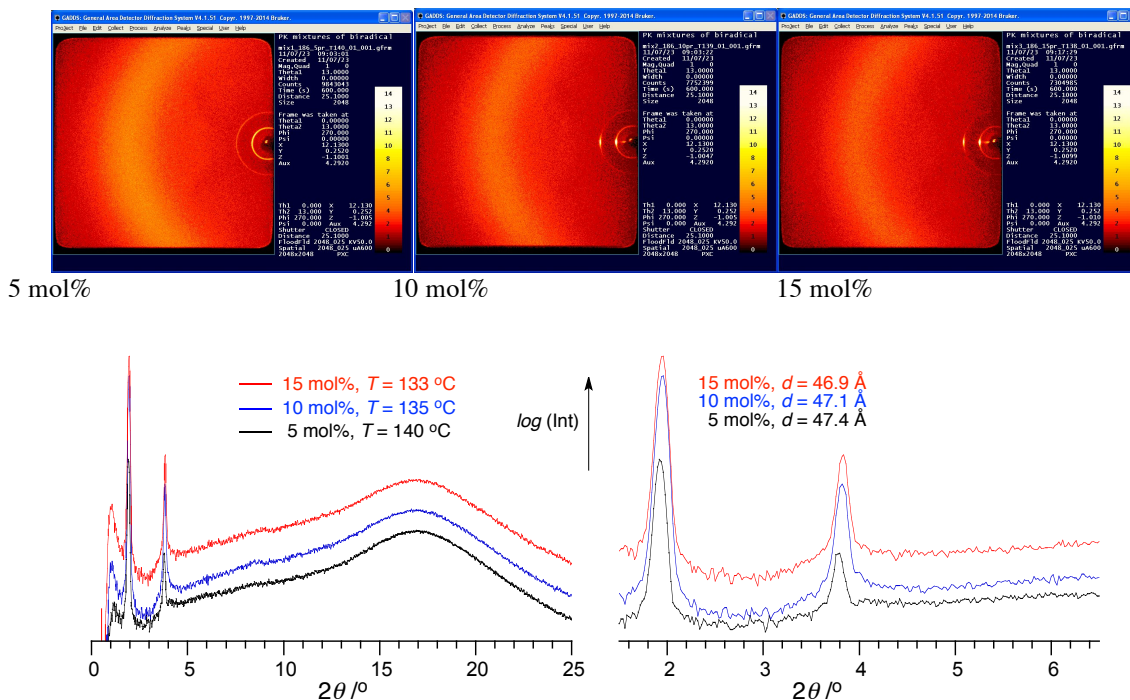


**Figure S19.** Top: 2D XRD patterns for 5, 10 and 15 mol% binary mixtures of 2[6,6] in host 1[8,6] taken at temperatures 10 K below the SmA-I transition. Bottom: X-ray diffractograms for 5, 10 and 15 mol% binary mixtures of 2[6,6] in host 1[8,6] obtained by integration of the 2D patterns presented above; the right panel shows zoomed low-angle range.



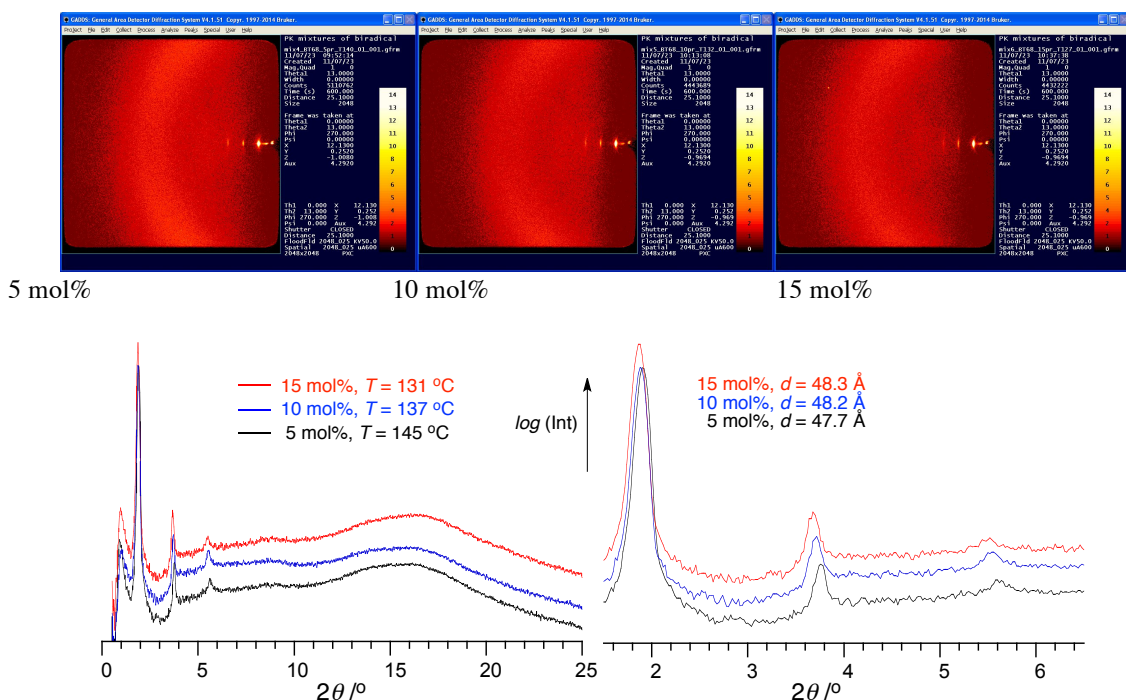


**Figure S20.** Top: 2D XRD patterns for 5, 10 and 15 mol% binary mixtures of **2[6,6]** in host **BT[6,8]** taken at temperatures 10 K below the SmA-I transition. Bottom: X-ray diffractograms for 5, 10 and 15 mol% binary mixtures **2[6,6]** in host **1[8,6]** obtained by integration of the 2D patterns presented above; the right panel shows zoomed low-angle range.

## 5. Computational details

### a) geometry optimization and PES scan

Quantum-mechanical calculations were carried out using Gaussian 09 suite of programs.<sup>2</sup> Geometry optimization of **3** was performed at the UB3LYP/6-31G(2d,p) level of theory in gas phase using tight convergence criteria and no symmetry constrains. Frequency calculations were performed to verify the nature of the stationary points and to obtain ZPE corrections for identified conformational minima. Zero-point energy (ZPE) corrections were scaled by 0.9806.<sup>3</sup>

Initially, the equilibrium geometry of triplet state **3-T-anti** in the anti-conformation of the 6-oxoverdazyl units was located through a limited conformational search. The obtained geometry was used as a starting point for a relaxed scan of the potential energy surface (PES) of **3-T**, in which the torsion angle  $\phi$  between the central benzene ring and one of the 6-oxoverdazyls was varied by 7.5° at a time. This resulted in an energy minimum

at  $\phi = -145^\circ$  corresponding to a local *syn* conformational minimum of **3-T**, which was further optimized through a limited conformational search giving the global conformational minimum **3-T-syn**. The equilibrium geometries for the triplet **3-T-anti** and **3-T-syn** were used as the starting points for geometry optimization of the analogous open-shell singlet structures, **3-OSS-anti** and **3-OSS-syn**. The former was used for a PES relaxed scan analogous to that of **3-T** shown in Figure S21. The broken symmetry (BS) formalism for geometry optimization of **3-OSS** was executed with the “guess(mix, always)” keyword.

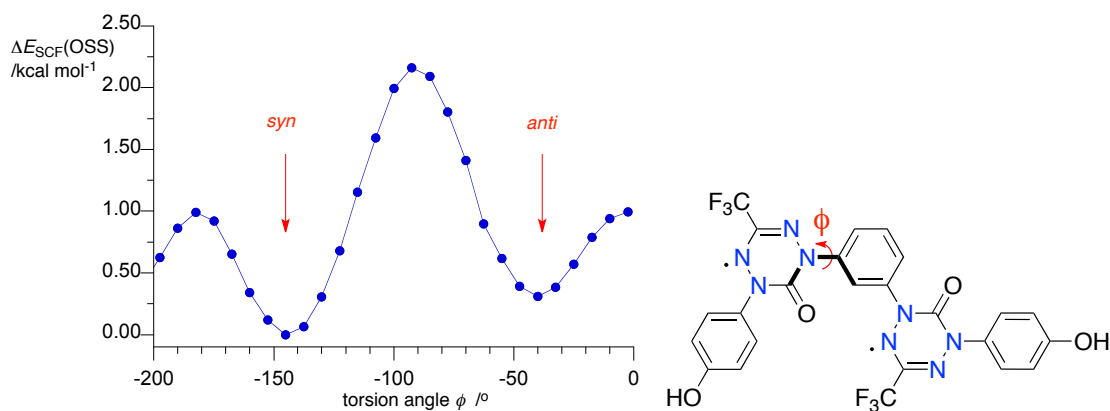


**Figure S21.** Relative SCF energy for PES scan for **3-OSS** with indicated torsion angle varied in the relaxed scan.

### b) singlet–triplet energy gap $\Delta E_{S-T}$

Adiabatic singlet-triplet energy gaps,  $\Delta E_{S-T}$ , for conformational minima **3-anti** and **3-syn** were calculated as a difference of  $E_S$  and  $E_T$  energies obtained using the UB3LYP/6-31G(2d,p) level of theory corrected for ZPE and the Yamaguchi formalism:<sup>4,6</sup>

$$\Delta E_{S-T} = 2J = 2 \frac{E_{BS} - E_T}{\langle S^2 \rangle_T - \langle S^2 \rangle_{BS}}$$

where the SCF energies of the triplet ( $E_T$ ) and broken symmetry singlet ( $E_{BS}$ ) corrected for ZPE and  $\langle S^2 \rangle$  represents the total spin angular momentum (of the T or OSS state) before spin annihilation.

The  $\Delta E_{S-T}$  values as a function of the torsion angle  $\phi$  were obtained in analogous way using SCF energies calculated for **3-T** and **3-OSS** for each value of the angle  $\phi$ .

## 6. Archive for DFT results

### 3-T-anti (triplet)

```
1\1\GINC-LOCALHOST\FOpt\UB3LYP\6-31G(2d,p)\C24H14F6N8O4(3)\PIOTR\07-Jun-2019\0\#\#P UB3LYP/6-31G(2d,p) Fopt(tight) #P geom(noangle, nodistance) fcheck freq(noraman, readIso)\1,3-Bis-[3-CF3-1-(4-HOphenyl)-6-oxoverdazl-5-yl]benzene, triplet or 2\0,3\N,2.0244131729,-0.1459562996,1.2766129551\N,4.6065631188,-0.4002916253,0.4215973391\C,5.9981510486,-0.5234434187,0.1020085509\C,6.9242739294,-0.4599160415,1.1492411351\C,8.2825334809,-0.5419851055,0.8886900513\C,8.7342685797,-0.688147016,-0.4258764755\C,7.8099104793,-0.7440580538,-1.4710299617\C,6.4467310511,-0.6602609064,-1.2136486032\C,1.2041490116,-1.5867484237,-0.4003435354\C,1.2881805874,-2.8616718694,-0.9661025958\C,0.1520763085,-3.412803603,-1.5500021573\C,-1.0543941026,-2.7246864983,-1.5703692053\C,-1.1264697194,-1.4573964511,-0.9864340415\C,0.0005414332,-0.8802830929,-0.4034564726\O,10.0771453073,-0.7687603556,-0.6224909947\C,-4.6690024159,1.4742768749,0.7973044084\C,-3.918965528,2.3397748464,1.5974807183\C,-6.0610526102,1.4327171197,0.9347483838\C,-4.5601656844,3.1460976869,2.5296303542\C,-6.697430483,2.2398820141,1.8637463335\C,-5.9488465721,3.1010615021,2.67075011\N,-3.1254036999,-1.022195388,-2.152891424\N,-4.0583244041,0.6492614634,-0.2016934803\O,-6.6248207867,3.865292148,3.5691827846\C,3.6317498062,-1.1333099181,-0.2725927348\C,-2.8081233628,0.0487480352,0.0183007931\O,3.8901293004,-1.8428781351,-1.2182748461\O,-2.1659213387,0.2079974782,1.0303449962\C,3.0558325302,0.4618637555,1.8237277286\C,-4.3007726857,-0.4265731744,-2.1761005342\N,2.3323427624,-0.9655488107,0.230238994\N,-2.3703087059,-0.7504267386,-1.0497988982\N,4.3330410072,0.3969966644,1.4898453584\N,-4.8279130198,0.4070009686,-1.2977367985\H,5.7420117371,-0.7048775001,-2.0299720691\H,8.1541585675,-0.8490657729,-2.4963152018\H,9.0075915793,-0.4989224261,1.6929000842\H,6.5683868029,-0.3368692758,2.1637518712\H,-0.0475316799,0.0916041516,0.0590729468\H,-1.9342968106,-3.1496660915,-2.0335846231\H,0.2090697991,-4.4023039782,-1.9898674906\H,2.2188274074,-3.4069615005,-0.9537173051\H,-2.8446386542,2.3817620218,1.5015011344\H,-6.63627398,0.7697920921,0.3020865177\H,-3.9717931245,3.81732115,3.1492312461\H,-7.7743453065,2.2115015838,1.9811262472\C,2.7470107745,1.4070585674,2.976222982\C,-5.1893697112,-0.7693248905,-3.3633147119\F,2.7819619541,2.6845422325,2.5578978586\F,3.6536566532,1.2777802184,3.9528387475\F,1.5388997803,1.1762778409,3.4889629426\F,-4.46418347,-1.107367951,-4.4320499517\F,-5.9856018381,-1.8123389059,-3.0632175549\F,-5.9757977764,0.2585478606,-3.6927113022\H,10.2551374869,-0.8659546368,-1.5649781985\H,-5.9972028571,4.4057527785,4.0625952152\Version=ES64L-G09RevD.01\State=3-A\HF=-2260.8893106\S2=2.03906\S2-1=0.\S2A=2.000877\RMSD=2.273e-09\RMSF=4.094e-07\Dipole=1.1375231,0.0909003,-0.0563757\Quadrupole=5.4969797,2.3629676,-7.8599473,-8.7767126,-22.6643921,5.3854295\PG=C01 [X(C24H14F6N8O4)]\
```

### 3-OSS-anti (open-shell singlet)

```
1\1\GINC-LOCALHOST\FOpt\UB3LYP\6-31G(2d,p)\C24H14F6N8O4\PIOTR\08-Jun-2019\0\#\#P UB3LYP/6-31G(2d,p) Fopt(tight) guess(mix, always) #P geom(noangle, nodistance) fcheck freq(noraman, readIso)\1,3-Bis-[3-CF3-1-(4-HOphenyl)-6-oxoverdazl-5-yl]benzene, singlet start at t2\0,1\N,2.0281904463,-0.1378232807,1.2782898679\N,4.6086070637,-0.3967025582,0.4176464913\C,5.9992747315,-0.5229541343,0.0959250363\C,6.9276775892,-0.455780557,1.1409613712\C,8.2852783875,-0.5407532369,0.8780054804\C,8.7341424323,-0.693585176,-0.4367955474\C,7.807558786,-0.7531529669,-1.4797873078\C,6.4450284441,-0.6664060443,-1.2200366576\C,1.203339936,-1.5863989772,-0.3902073893\C,1.2846594418,-2.8667793487,-0.9426330561\C,0.1477682257,-3.4219037149,-1.5212472824\C,-1.0572905706,-2.7313100568,-1.5
```

481449515\C,-1.1260061647,-1.4585392125,-0.9775931181\C,0.0017338613,-  
0.8773032906,-0.4010722847\O,10.0764947022,-0.7768472702,-0.635763703\  
C,-4.6743737316,1.4700161055,0.7983605444\C,-3.9272841385,2.3272893366  
,1.6101446265\C,-6.0676532564,1.4331599733,0.9245390594\C,-4.5726958,3  
.1301074837,2.5424003433\C,-6.708176645,2.236832772,1.8537158639\C,-5.  
9626236754,3.0897749541,2.6721972688\N,-3.1160180031,-1.0126212981,-2.  
1568222995\N,-4.0589492707,0.6492747641,-0.2010397109\O,-6.6426844786,  
3.8509251506,3.5701821506\C,3.6310112969,-1.1318759749,-0.2715307545\C  
, -2.8115779866,0.0435991923,0.0238650967\O,3.88656966,-1.845054121,-1.  
2152534458\O,-2.1756596399,0.1941864602,1.0411711447\C,3.0612386866,0.  
4707255501,1.8209584556\C,-4.2895767746,-0.4138380725,-2.1844802294\N,  
2.3340057431,-0.9620148401,0.2345162032\N,-2.3688983089,-0.7489153312,  
-1.0461029835\N,4.3378771725,0.4038702835,1.4839032761\N,-4.820981189,  
0.4153301792,-1.3040290717\H,5.7385718977,-0.7138557578,-2.0346935006\  
H,8.1495686469,-0.8633366589,-2.505278021\H,9.0120319313,-0.49494619,1  
.680532333\H,6.5740366823,-0.3277325973,2.1556390249\H,-0.0449865497,0  
.099329533,0.0519698841\H,-1.9383762091,-3.1588235861,-2.0070370858\H,  
0.2029381665,-4.4157969893,-1.9512924044\H,2.214434312,-3.4135958445,-  
0.9245722442\H,-2.8520703463,2.3655167876,1.5229931667\H,-6.6404183401  
,0.7766537333,0.2830252664\H,-3.9866205394,3.7949279344,3.1710179413\H  
, -7.7860960002,2.2120216377,1.9623715064\C,2.7568985758,1.4195206202,2  
.9716451872\C,-5.1709488436,-0.7462740433,-3.3799519618\F,2.8022888465  
,2.6961939647,2.552063628\F,3.660691559,1.2845048784,3.9502596174\F,1.  
5461649158,1.1982087021,3.4822423238\F,-4.4394679121,-1.0816311513,-4.  
445198236\F,-5.9738973614,-1.7873926073,-3.0913478352\F,-5.9505498837,  
0.2868191853,-3.709423268\H,10.2524507035,-0.8786083548,-1.5781528328\  
H,-6.0168560951,4.3856812616,4.072012644\\Version=ES64L-G09RevD.01\Sta  
te=1-A\HF=-2260.889054\S2=1.035324\S2-1=0.\S2A=0.287435\RMSD=5.163e-09  
\RMSF=5.755e-07\Dipole=1.1363011,0.0732902,-0.0468856\Quadrupole=5.561  
5476,2.3143431,-7.8758907,-8.7871269,-22.7043388,5.4403092\PG=C01 [X(C  
24H14F6N8O4)]\

### 3-T-syn

1\1\GINC-LOCALHOST\FOpt\UB3LYP\6-31G(2d,p)\C24H14F6N8O4(3)\PIOTR\30-Au  
g-2023\0\#\#P UB3LYP/6-31G(2d,p) Fopt(tight) #P geom(noangle, nodistanc  
e) fcheck freq(noraman, readIso)\1,3-Bis-[1,3-bis(4-MeOphenyl)-6-oxov  
erdazl-5-yl]benzene, glob min syn\0,3\N,2.1707300749,0.4644667307,1.0  
769323315\N,4.6706924562,-0.268096734,0.2485560523\C,6.00056928,-0.515  
2259822,-0.2219883315\C,6.7868932835,0.580604368,-0.5953635517\C,8.092  
0629613,0.3934763135,-1.0207392682\C,8.6299661376,-0.8951074722,-1.079  
1418171\C,7.846440512,-1.987899774,-0.7017734498\C,6.5377827269,-1.803  
6520695,-0.2727389625\C,1.1857556189,-1.4903178863,0.2034397799\C,1.19  
28786945,-2.8876518447,0.2132946583\C,-0.0030840251,-3.5659825905,0.00  
51911293\C,-1.1983625007,-2.8872342235,-0.2054690145\C,-1.1898289138,-  
1.489880665,-0.2008779332\C,-0.0016827839,-0.7892520753,-0.0000383239\  
O,9.9136952659,-1.0206947984,-1.5087351505\C,-6.0036578353,-0.50833507  
59,0.2208437613\C,-6.5421863138,-1.7960129995,0.2763952764\C,-6.788857  
9772,0.5896821096,0.5901334974\C,-7.8510289742,-1.9773235898,0.7061158  
121\C,-8.0942157529,0.4054751319,1.0162062954\C,-8.6334346914,-0.88233  
18511,1.079411053\N,-2.1728281391,0.462601716,-1.0817173557\N,-4.67353  
24366,-0.2643204539,-0.25062123\O,-9.9172890873,-1.0050054585,1.509472  
5362\C,3.6173005461,-1.1459447871,-0.0529099718\C,-3.6210300415,-1.142  
0952879,0.0541481363\O,3.7684907772,-2.1684647081,-0.6821161864\O,-3.7  
732610303,-2.1620944844,0.6871837968\C,3.2531327859,1.1959048652,1.231  
8670085\C,-3.2544917722,1.1945432004,-1.2394135945\N,2.3746602555,-0.7  
296564713,0.4481787455\N,-2.3779659504,-0.7289443176,-0.4484814977\N,4  
.4991912329,0.9227470464,0.8839090325\N,-4.5008280336,0.9239522135,-0.  
8904456406\H,5.9416561969,-2.6565328166,0.0143891532\H,8.2603382585,-2

.991970317,-0.7385508188\H,8.7075085899,1.234979627,-1.3163290229\H,6.367309181,1.5764268597,-0.5396529379\H,-0.0011380078,0.2900566698,-0.0020701643\H,-2.1177840417,-3.4294875035,-0.363176325\H,-0.0036309793,-4.6503673065,0.007234107\H,2.1117525801,-3.4302349251,0.3730466997\H,-5.9469325231,-2.6505657448,-0.0075551106\H,-6.3682559068,1.5848605088,0.5307103151\H,-8.2659533623,-2.9808262347,0.7466350288\H,-8.7087998828,1.2487023113,1.3086590693\C,3.0774628045,2.5290466984,1.9449570625\C,-3.0774711548,2.524816572,-1.9575086743\F,3.6288767017,3.5207014675,1.2307413081\F,3.6838498681,2.508184866,3.1420248695\F,1.7901895883,2.8162090462,2.1366192908\F,-1.7899079746,2.8099492269,-2.1502493162\F,-3.6838855386,2.500073329,-3.1544880607\F,-3.6278752359,3.5197071542,-1.2470224514\H,10.1605268532,-1.9525882565,-1.5042513148\H,-10.1650772945,-1.9366552965,1.5084495797\Version=ES64L-G09RevD.01\State=3-A\HF=-2260.8900918\S2=2.039028\S2-1=0.\S2A=2.000878\RMSD=3.445e-09\RMSF=2.585e-07\Dipole=-0.001185,-2.3179686,0.0043352\Quadrupole=26.4847368,-5.0907597,-21.3939771,-0.0301302,-7.5571555,-0.0265891\PG=C01 [X(C24H14F6N8O4)]\

### 3-OSS-syn

1\1\GINC-LOCALHOST\FOpt\UB3LYP\6-31G(2d,p)\C24H14F6N8O4\PIOTR\30-Aug-2023\0\#\#P UB3LYP/6-31G(2d,p) Fopt(tight) guess(mix, always) #P geom(no angle, nodistance) fcheck freq(noraman, ReadIso)\1,3-Bis-[1,3-bis(4-MeOphenyl)-6-oxoverdazl-5-yl]benzene, glob min syn, start at T\0,1\N,2.1712394787,0.4624960331,1.0816150198\N,4.6710936901,-0.2684356659,0.2503384699\C,6.0005450065,-0.5143153928,-0.2217178358\C,6.787276812,0.5826374404,-0.5910422357\C,8.0921772997,0.3966068672,-1.0176895279\C,8.629465184,-0.8919852304,-1.0814810517\C,7.8455692156,-1.98591033,-0.7081918105\C,6.5371793535,-1.802792172,-0.2778667486\C,1.1852636167,-1.4903983469,0.2042059212\C,1.1924855699,-2.8872375706,0.214426106\C,-0.0030858335,-3.5659089825,0.0051644563\C,-1.1979714944,-2.8868206547,-0.2066458403\C,-1.1893385837,-1.4899609018,-0.2016697216\C,-0.0016834305,-0.789168431,-0.0000477857\O,9.9129608806,-1.016436232,-1.5120987746\C,-6.0036303998,-0.5074204936,0.2205789522\C,-6.541566777,-1.7951342829,0.2815644899\C,-6.7892521058,0.5917059493,0.5857810844\C,-7.8501400019,-1.9753127951,0.7125723503\C,-8.0943388918,0.4085976897,1.0131221684\C,-8.6329288793,-0.8792020494,1.0817507117\N,-2.1733426705,0.4606207077,-1.086406193\N,-4.673932433,-0.2646587061,-0.25239552\O,-9.9165486454,-1.0007379257,1.5128309823\C,3.6167149711,-1.1451565682,-0.0535023957\C,-3.6204395097,-1.1412978898,0.054735968\O,3.7676060881,-2.1657224963,-0.6859600446\O,-3.7723600461,-2.1593283381,0.6910218984\C,3.2539414397,1.1925212765,1.239427728\C,-3.2553067849,1.1911419177,-1.2469603512\N,2.3752884119,-0.7302409245,0.4496462739\N,-2.3785953455,-0.7295285535,-0.4499645377\N,4.5000679005,0.9198366736,0.8902382198\N,-4.5017073726,0.921029476,-0.8967515826\H,5.9407831612,-2.6565265504,0.0061145122\H,8.2589814079,-2.9900196126,-0.7491529941\H,8.7078766749,1.2389993037,-1.3102062333\H,6.3681685953,1.5784249182,-0.5312422047\H,-0.0011382955,0.2901697888,-0.0020738421\H,-2.1173952124,-3.428909822,-0.3652896202\H,-0.0036334976,-4.6502817186,0.0071999212\H,2.1113615766,-3.4296557611,0.375105577\H,-5.9460346127,-2.6505313002,0.0007914124\H,-6.3691377076,1.586837735,0.5222432386\H,-8.2645668514,-2.9788428107,0.757302712\H,-8.7091857043,1.2527044086,1.3024731763\C,3.0792136531,2.523573091,1.9565793338\C,-3.0792356798,2.5193149415,-1.9691033746\F,3.6295391702,3.5172916549,1.2443443488\F,3.6873635592,2.4993703482,3.1526764085\F,1.7922168227,2.8101078573,2.1508885806\F,-1.7919504644,2.8038168196,-2.1644864071\F,-3.6874139211,2.4912374324,-3.1651013321\F,-3.6285536493,3.5162560531,-1.2606037673\H,10.1592690997,-1.94847939,-1.5117354127\H,-10.163798768,-1.9325264538,1.5159670335\Version=ES64L-G09RevD.01\State=1-A\HF=-2260.8898412\S2=1.035044\S2-1=0.\S2A=0.286943\RMS

D=3.625e-09\RMSF=2.644e-07\Dipole=-0.0011706,-2.3168798,0.0043488\Quadrupole=26.4580024,-5.0225055,-21.4354969,-0.0302927,-7.6661899,-0.0269392\PG=C01 [X(C24H14F6N8O4)]\

## 7. References

- 1 G. A. Bain, J. F. Berry, *J. Chem. Ed.*, 2008, **85**, 532–536.
- 2 Gaussian 09, Revision A.02, M. J. Frisch, G. W. Trucks, H. B. Schlegel, G. E. Scuseria, M. A. Robb, J. R. Cheeseman, G. Scalmani, V. Barone, B. Mennucci, G. A. Petersson, H. Nakatsuji, M. Caricato, X. Li, H. P. Hratchian, A. F. Izmaylov, J. Bloino, G. Zheng, J. L. Sonnenberg, M. Hada, M. Ehara, K. Toyota, R. Fukuda, J. Hasegawa, M. Ishida, T. Nakajima, Y. Honda, O. Kitao, H. Nakai, T. Vreven, J. A. Montgomery, Jr., J. E. Peralta, F. Ogliaro, M. Bearpark, J. J. Heyd, E. Brothers, K. N. Kudin, V. N. Staroverov, R. Kobayashi, J. Normand, K. Raghavachari, A. Rendell, J. C. Burant, S. S. Iyengar, J. Tomasi, M. Cossi, N. Rega, J. M. Millam, M. Klene, J. E. Knox, J. B. Cross, V. Bakken, C. Adamo, J. Jaramillo, R. Gomperts, R. E. Stratmann, O. Yazyev, A. J. Austin, R. Cammi, C. Pomelli, J. W. Ochterski, R. L. Martin, K. Morokuma, V. G. Zakrzewski, G. A. Voth, P. Salvador, J. J. Dannenberg, S. Dapprich, A. D. Daniels, O. Farkas, J. B. Foresman, J. V. Ortiz, J. Cioslowski, and D. J. Fox, Gaussian, Inc., Wallingford CT, 2009.
- 3 A. P. Scott, L. Radom, *J. Phys. Chem.*, 1996, **100**, 16502-16513.
- 4 K. Yamaguchi, *Chem. Phys. Lett.*, 1975, **33**, 330–335.
- 5 K. Yamaguchi, Y. Takahara, T. Fueno, K. Nasu, *Jpn. J. Appl. Phys.*, 1987, **26**, L1362-L1364.
- 6 K. Yamaguchi, F. Jensen, A. Dorigo, K. N. Houk, *Chem. Phys. Lett.*, 1988, **149**, 537–542.